PHYSIOLOGY REVIEWS
Vol. FF, No. 6, Jan. 2020

Osteogenic Marrow Treatment via Cell-BSMC Stromal Stimulation Therapy

Daniel K. Salzburg[1] | **Antonia I. Allard**[2]

[1]Department of Applied Theory, University of Salisbury, USA

Correspondence
Daniel K. Salzburg, Department of Applied Theory, University of Salisbury, USA
Email: daniel.salzburg@sixsixsigma.com

Funding information
Yuhan Grant/Award Number: YUHPN1J0C1C1, Environmental Protection Agency Grant/Award Number: EPA6H78T1H1W1W1, Parke-Davis Grant/Award Number: PAR225413W52325

In vitro cultures of MDSCs and hMSCs induce proliferation and differentiation of bone marrow-derived mesenchymal stem cells, endothelial-derived or endothelial-derived stromal cells, mesenchymal stem cells (MSCs), and adipose-derived progenitor cells. These studies demonstrate the potential for using MDSCs in clinical applications. The primary goal of this work was to investigate the use of MDSCs and hMSCs in large animal wound healing models. Using cell-based therapies, the goal was to improve outcomes with a combination of cell types. Cells seeded into the appropriate conditions were used in these studies, where cells were used for treatment of chronic wounds and in conditions that involve cell replacement.

Animals and Methods All animal experiments were approved by the Stanford University Animal Care and Use Committee. MDSCs and hMSC cultures were maintained under identical conditions in a 37°C incubator. All experimental procedures complied with the guidelines set forth by the NIH guidelines for animal experimentation and were in accordance with the standards of the National Institutes of Health (NIH Publication No. All animal procedures were in accordance with the guidelines for the humane care and use of laboratory animals developed by the University of California, San Diego, National Institutes of Health, and the Stanford University Animal Care and Use Committee (1988–1994). MDSCs and hMSCs were maintained in a 37°C incubator under standard laboratory animal care procedures. MDSCs were maintained in serum-free DMEM media supplemented with 1% penicillin/streptomycin in the presence of 1X EGTA (Sigma-Aldrich Corp., St Louis, MO, USA), in DMEM medium for 30 days. The culture medium was changed every three days, and the amount of serum was kept at a constant constant amount (2–3 × 10 6 cells/ml). MDSCs and hMSCs were maintained in DMEM media supplemented with 1% penicillin/streptomycin, in DMEM medium for 30 days. The media was changed weekly, and the media was replaced weekly. Animal procedures were in accordance with the NIH guidelines for the humane care and use of laboratory animals. All animal experiments were performed in compliance with the guidelines of the National Institutes of Health in accordance with the Animal

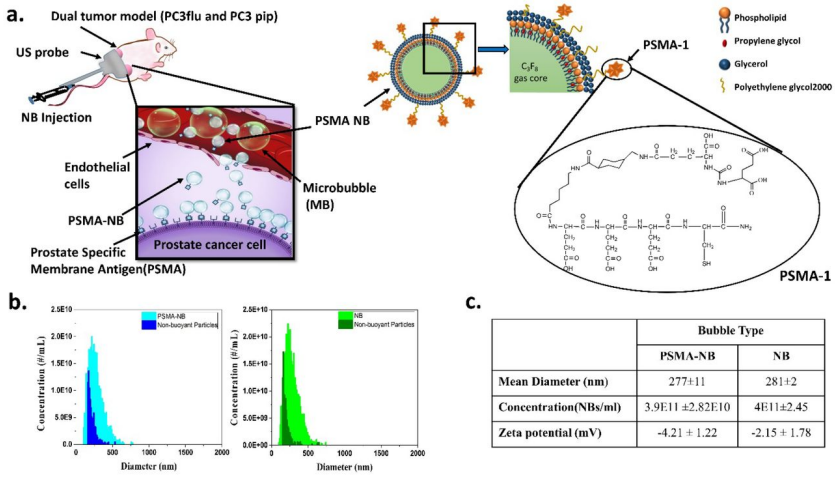

	Bubble Type	
	PSMA-NB	NB
Mean Diameter (nm)	277±11	281±2
Concentration(NBs/ml)	3.9E11 ±2.82E10	4E11±2.45
Zeta potential (mV)	-4.21 ± 1.22	-2.15 ± 1.78

FIGURE 1 Visualization of Humidified Microbubbles

Care and Use Committee of the National Institute of Health (11–6–year) and with approval of the Stanford University Animal Care and Use Committee (12–year) (NIH Publication No.

The number of cells in culture media was determined by counting the number of cells in the media with and without exogenous gene transfer (Figure 2). The number of cells in culture media was determined for each of the three stages of wound healing (Figure 4).

We examined the effects on bone healing by comparing the number of osteoblasts in the wounds of animals treated with exogenous gene transfer with untreated wounds (Figure 10). The number of osteoblasts decreased significantly in wounds treated with exogenous gene transfer and significantly decreased in wounds treated with both control and exogenous gene transfer (Figure 6). We found that exogenous gene transfer significantly decreased the number of osteoblasts in wounds treated with control gene transfer. Exogenous gene transfer resulted in a decrease in osteoblast number in the wounds of animals treated with control gene transfer (Figure 7).

The bone healing ability of animals treated with exogenous gene transfer was significantly improved (Figure 2) compared with those treated with either control or exogenous gene transfer untreated wounds (Figure 3). Exogenous gene transfer significantly improved bone healing compared with control treatment in wound healing animals without exogenous gene transfer or treated with both control and exogenous gene transfer. Exogenous gene transfer significantly improved the healing ability of animals treated with control and exogenous gene transfer compared to wounds treated with both control and exogenous gene transfer, both using the same scaffolds. Exogenous gene transfer reduced the number of osteoblastic cells by an approximately 2-fold (Figure 3) compared to animals treated with control and exogenous gene transfer. Exogenous gene transfer significantly reduced the number of non-osteoblastic cells by an approximately 2-fold (Figure 4) as compared to wounds treated with control and exogenous gene transfer. Exogenous gene transfer significantly reduced the number of osteoblastic cells by an approximately 2-fold (Figure 10) compared to wounds treated with control and exogenous gene transfer, again using the same scaffolds. Exogenous gene transfer resulted in a decrease in osteoblastic cells in wound healing wounds of animals treated with untreated wounds compared to wounds treated with control or exogenous gene transfer.

In both control and exogenously treated wounds, the number of cells in the culture media increased significantly (Figure 2) compared with untreated wounds. Exogenous , the percentage of osteocytes was decreased in the treated

wounds of animals that received Pten-overexpressing control gene cells (Figure 8 , P>0.05). Interestingly, significant decrease in total osteoblast number was observed in wound healing in animals treated with Pten-overexpressing control gene transfer (Figure 9 , P<0.0001). However, the percentage of osteoblasts that expressed osteocalcin (arrows in Figure 9) was significantly decreased in wounds treated with control gene transfer. The percentage of osteocytes that co-expressed osteocalcin did not change in wounds treated with Pten-overexpressing control gene transfer.

The bone marrow stromal cells (BMSCs) are a key component of the endogenous and lentiviral mediated gene transfer system. The mechanism of bone marrow stromal cell–BMSC interaction is mediated by VEGF, which is a potent osteogenic stimulator, providing a potential avenue for therapeutic application in the treatment of osteoporotic diseases (Pagni et al. (2013)). The purpose of the present study was to determine the effect of VEGF gene transfer on the interaction of the bone marrow stromal cells and the bone marrow stromal cells with the BMSCs and BMSC mononuclear cells in vitro , and whether the effect of Pten-overexpressing control genes on these interactions can be reversed in the treated wounds of BMSCs and BMSC mononuclear cells.

The current study was designed to examine the effect of gene transfer on the differentiation of the BMSCs, BMSCs and mononuclear cells, and the interactions of the two groups of cells in vitro . The purpose was to determine the effect of Pten-overexpressing control genes on the differentiation of BMSCs, BMSCs and mononuclear cells in vivo . In addition, the results of this study were to determine their effect on BMSC or BMSC mononuclear cell characteristics.

Steratin (Steratin), an activator of mitosis, has been shown to be a powerful activator of bone formation (Lee et al. (2010)). However, the activity of the secreted soluble soluble isoform of the vasodilatase has not been determined and the effects of the soluble soluble isoform on the differentiation of BMSCs and BMSC mononuclear cells has not been determined. Based on the present study, we hypothesized that the effects of Pten–overexpressing control genes on the differentiation and cell differentiation of BMSCs and BMSC mononuclear cells would be more pronounced and efficient when compared to the effects of Pten-overexpressing control genes. This would be particularly helpful in cases of severe and repeated burn injuries in which the cell is inactivated, and in cases of poor survival of BMSCs in vivo .

The biological effects of Pten–overexpressing control gene transfer were determined by measuring the effects of total gene expression in the wound. Based on the present study, we hypothesized that the effects of Pten–overexpressing control genes on the differentiation and cell differentiation of BMSCs and BMSC mononuclear cells would be more pronounced and efficient when compared to the effects of Pten-overexpressing control genes. The mechanisms of these effects, which we analyzed and compared, included: (Huang et al. (2015)) the effect of the Pten–overexpressing control genes on the cell morphology of the wound, (Sen et al. (2013)) the effect of the Pten–overexpressing control genes on the cell proliferation, (ad (2010)) the effect of the Pten-overexpressing control genes on cell death, (Liu et al. (2013)) the effect of the Pten-overexpressing control genes on cell apoptosis.

Since our studies aimed to determine the effect of Pten–overexpressing control genes on the cell proliferation in vitro , we also hypothesized that the effect of Pten-overexpressing control genes on the cell proliferation in vivo . The results of this study were based on our quantitative analysis of the effects of Pten-overexpressing gene transfer on the cell differentiation and cell proliferation of the wound, a critical component of the endogenous and lentiviral mediated bone marrow stromal cell–BMSC interaction.

Cell culture The wound was harvested at 28-day-old male nude mice with wounds in the center of each center and the outer margin of the wound area. The wound was then collected into 4-mL glass pipettes and frozen in liquid nitrogen. The wound was flushed with PBS and a series of 5-μm-thick, 0.1-μm-thick, 1-μm-thick, and 2-μm-thick frozen-wells were then placed in aseptic-fixed fixatives (Figure 2). At the skin was washed and then in 4-mL phosphate-buffered by potential therapies may involve delivery of precommitted BMSC progenitors to be used to

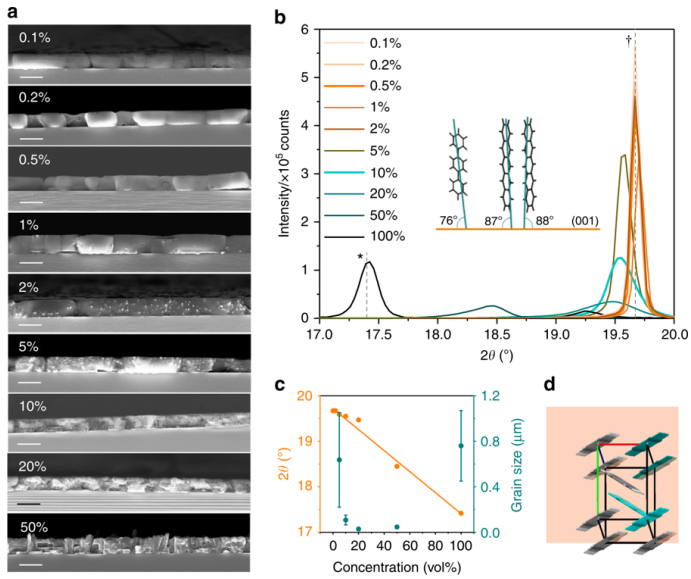

FIGURE 2 Approximate Osteoblastic Exogenous Transfer.

promote regenerative processes.

Skeletal muscle is a key component of the host body, where it is vital to maintain bodyweight and mobility during the homeostatic response of the organism. Despite recent advances in the use of cell-based therapeutics, such as tissue and protein delivery, it is still unclear how the cells are delivered to the target tissue. For example, in the case of muscle biopsy of burned skeletal muscle, delivery of skeletal muscle stem cells with the goal of promoting regeneration is still under development. In addition, the regenerative capacity of muscle in burned rats has not been established, but the ability to regenerate muscle after injury would aid the use of these cells in the long term. The first reports of a muscle-intrinsic therapy for type II diabetes mellitus have focused on the development of an injectable autologous stem cell product. The aim has been to develop a delivery system to increase the number of cells sufficient to generate a large enough quantity for clinical use. This product will provide a long-term (7.4 years) survival of the diabetic and non-diabetic populations and will also provide a significant benefit over currently available treatment modalities. In order to improve the effectiveness of this therapy, strategies to direct the production of autologous stem cells from autologous or allogeneic sources are needed. Several studies have shown efficacy of autologous stem cell therapy for diabetic and nondiabetic muscle that is limited to preclinical studies. Therefore, it is not possible to establish a clinical trial using autologous stem cell therapy for the treatment of type II diabetes mellitus.

Recently, we reported that autologous stem cell therapy could be an effective therapy for diabetic and nondiabetic muscle that is limited to preclinical studies. Our group demonstrated that autologous stem cell therapy delivered to the diabetic myocardium improved the survival of the diabetic donor population and improved the overall functional outcome of the patient. The study was published in the March 2007 issue of the International Journal of Experimental Medicine, a journal of the International Society for Cellular Therapy.

Recent years have seen a dramatic emergence of new research tools within the field of diabetic biology. The discovery of diabetic streptozotocin, the first example of a diabetic drug, has contributed to advances in the understanding of the underlying pathophysiological processes in these conditions. The use of molecular biomarkers to track

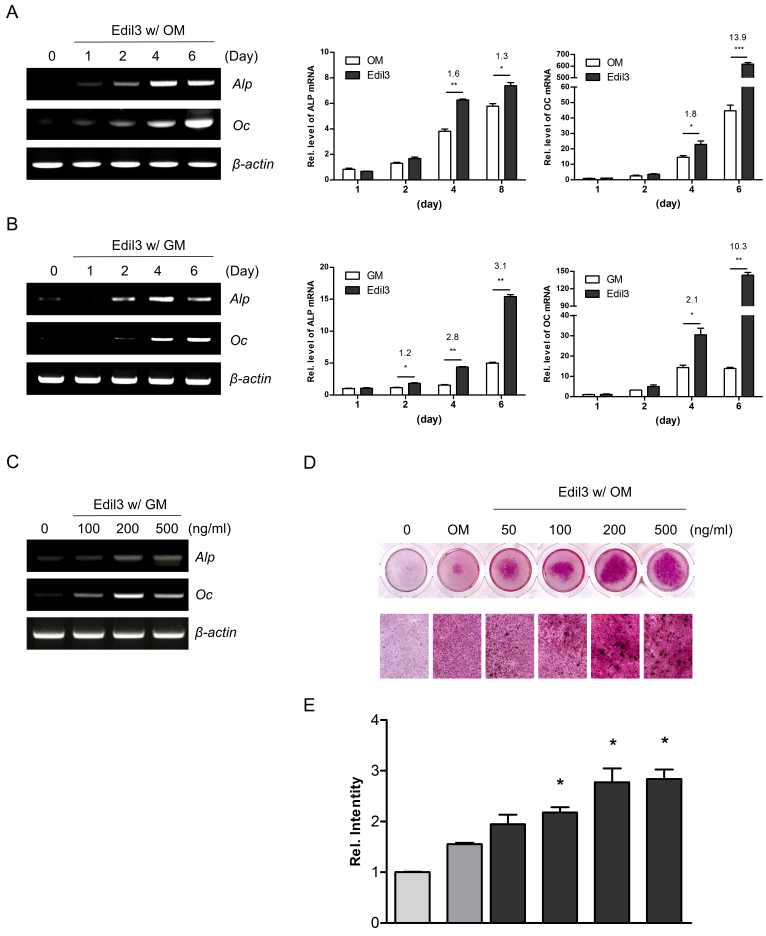

FIGURE 3 Approximate Non-osteoblastic Exogenous Significance

diabetic gene expression provides a novel means for the identification of cells that respond to disease and is an important new avenue for the study of diabetic complications and diseases. By using genetic information to identify these cells, the scientific community can provide insight into the development, progression, and maintenance of the diabetic genome.

In the past decade, a tremendous amount of progress has been made in identifying the etiology of diabetes. The use of genome-wide comparative genomics and genome-wide association study (GWAS) has been used to identify genes that are associated with diabetes, the etiology of diabetes, and pathophysiology of the disease from early embryos to the present day (reviewed in (Cai et al. The use of such large-scale studies has been extremely helpful in identifying the etiology of diabetes. For example, the use of such large-scale studies has been used to identify the etiology of most of the metabolic disease in the human body and to provide insight into the progression of diabetic complications in the body.

In the diabetic field, the use of genetic markers has been used to identify the etiology of many of the metabolic diseases, including type I diabetes (Type I diabetes, also known as DiI, is an inflammatory diabetic condition that is

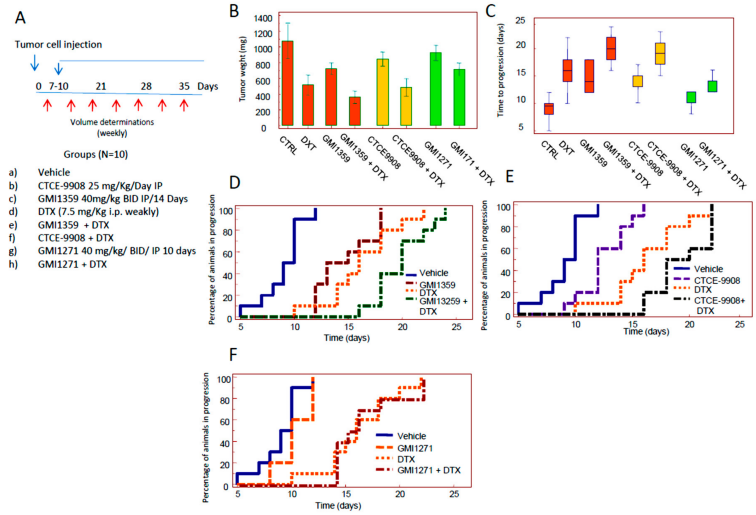

FIGURE 4 Approximate Non-osteoblastic Exogenous Scaffold Significance

often a fatal side effect of diabetes therapy) (Cai et al. The use of these approaches has been important to develop clinical trials or preclinical therapies with the goal of improving the success of treatment in diabetes. The use of genetic markers has been used to identify the etiology of many of the metabolic diseases, including type I diabetes. More recently, the use of genetic markers has been combined with autologous cells to provide a large-scale, rapid delivery, and therapeutic delivery.

The current generation of diabetic tissue autologous cells (DACCs) are currently in preclinical development. DACCs are delivered in various cell-cell contact interfaces, such as microbubbles of various ages and compositions and in vivo cell-cell interfaces (reviewed in (Dezawa et al. However, the use of autologous cells for the treatment of diabetes is currently quite limited in the field of DACCs. Autologous DACCs have the potential to be used in the clinic for diabetic complications.

The DACCs are the most widely used autologous cell-based therapy for the diabetic patients and are a patient is the most demanding. Diabetes is the most demanding, however, the patients require more time and the ice expressing VEGFR-3 (vWF) within the blood vessels had decreased endothelial cell number and enhanced expression of VEGFR-3 (p-expression) in vitro , demonstrating that the VEGFR signaling pathway may be important for endothelial cell differentiation into distinct and distinct endothelial progenitor lineages. Recent studies implicate VEGFR-3 as a key regulator of endothelial cell differentiation (Zhang et al.

Vascular endothelial growth factor (VEGF) is a key regulator of endothelial cell proliferation, migration, and angiogenesis, which are the key steps in the development and maintenance of a healthy endothelium (Zhang et al. The importance of VEGF in directing the progression of endothelial progenitor cells into the mature vasculature is demonstrated by the study of the effects of VEGF treatment on angiogenesis (Zhang et al. In this study, a combination of microbubbles (Fc receptor and VEGFR-3) from various preparations were injected into the hind limbs of pregnant mice, and their VEGF-containing microbubbles were applied in the right and hind limbs of a mouse contused with the VEGF-loaded microbubble scaffolds. VEGF treatment promoted cell proliferation and enhanced angiogenesis in the right hind limb of the pregnant mice. The combination of microbubbles and VEGF therapy in the hind limb demonstrated that VEGFR-3-positive endothelial progenitors were more vascularized, and the treatment significantly

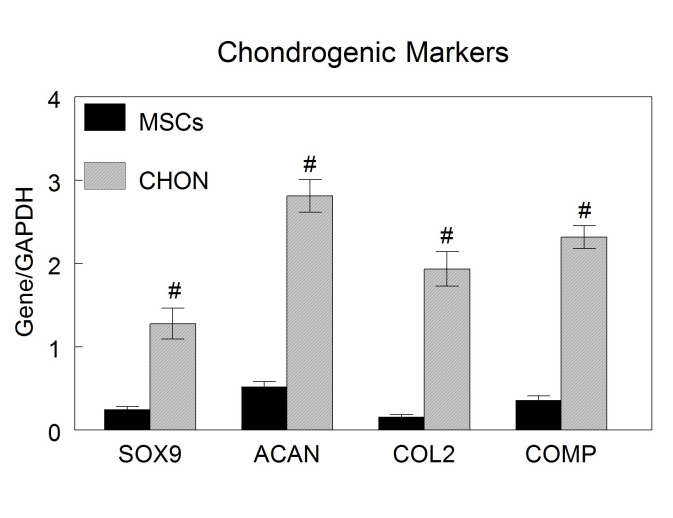

FIGURE 5 Decreased Significance in Exogenous Osteoblast Formation

improved blood flow recovery at 7 days compared to saline-treated mice. The combination of VEGFR-3-positive cells and microbubbles enhances angiogenesis significantly in mice contused with VEGF-loaded microbubbles. VEGFR-3 is a key regulator of endothelial cell development and maintenance and promotes vascular cell proliferation (Zhang et al.

The endothelial cell (EC) niche is a dynamic interplay of multiple cellular processes, including proliferation, migration, and remodeling (Li et al. The EC niche regulates cellular proliferation, migration, and angiogenesis, and is responsible for the maintenance of the integrity of blood flow, as well as the maintenance of the ability of a vessel to support blood flow (Zhang et al. The balance of pro- and anti-angiogenic factors is important in the regulation of the EC niche. Recent studies have demonstrated that VEGFR-3 expression was significantly decreased in the blood of ECs from pregnant mice, and the reduction in VEGFR-3 expression in ECs was associated with a decrease in blood flow recovery (Zhang et al.

Tissue sections from the hind limb of pregnant mice injected with VEGF-containing microbubbles were imaged by fluorescence microscopy. The number of VEGFR-3-positive endothelial cells per section was quantified by counting the number of endothelial cells in the hind limb of the injection group, and the ratio between the number of VEGFR-3-positive cells and the total number of VEGFR-3-positive endothelial cells in the hind limb of the control group. The amount of VEGFR-3 protein was measured by measuring the ratio of the ratio of the protein-to-phosphorylated vWF protein in 5 mL of phosphate buffered saline.

In order to determine the effects of VEGF treatment on the vascular cell proliferation and proliferation of the ECs in culture, a single-cell lysate lysis assay was run. The cells were lysed in 24-well plates, and the number of new endothelial cells per well was determined with an ELISA kit (RD Systems) according to manufacturer's instructions. The cells were lysed and then analyzed for VEGF expression.

ECs were transfected with either VEGFR-3 or VEGFR-3 siRNA using standard primers and the following primers: VEGFR3 floxed, Cdkn1b or Cdkn1a (green fluorescent protein), VEGFR3/ATP-coupled receptor (green fluorescent protein), VEGFR3 plasmid, or Tie2 (control). The transfected cells were then injected intraperitoneally and used for studies. The numbers of VEGFR-3-positive cells counted per section were normalized to total VEGFR-3 protein.

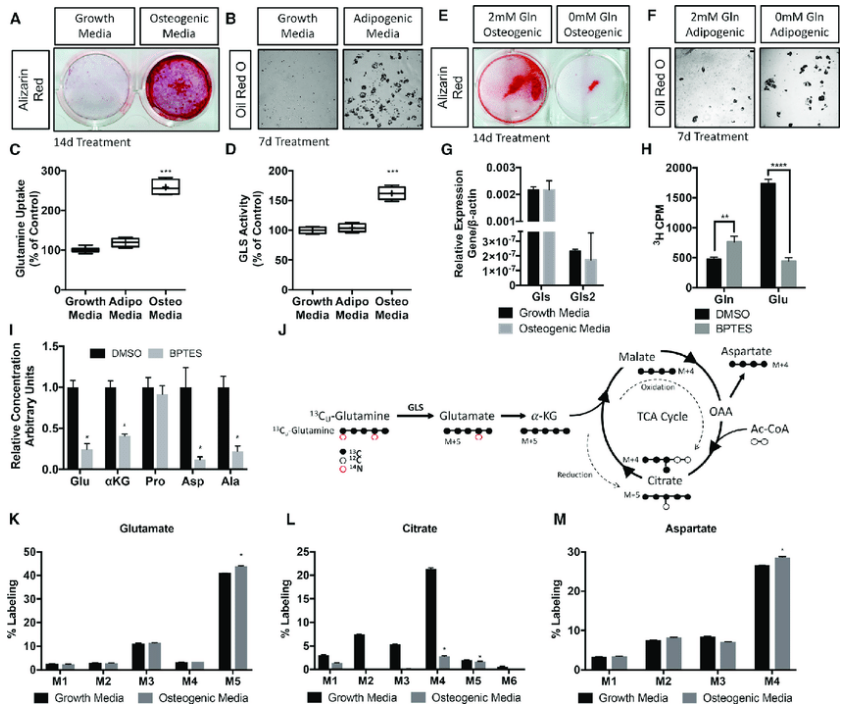

FIGURE 6 Resultant Osteoblast Exogenous Transfer

After 3 and 7 days of culture, tissues were fixed with 4% paraformaldehyde (Sigma-Aldrich, St. Louis, MO) for 20 minutes, and paraffin-embedded tissue was sectioned and stained with hematoxylin and eosin (HE). The number of myeloid cells per tissue section was counted to determine the area of VEGF-containing microbubbles was measured using an image analysis system (Image-Pro Plus imaging software, Media Cybernetics).

Histological analysis of embryos injected with VEGF-containing microbubbles in vitro was based on the amount of VEGF-containing microbubbles injected at the time of delivery. At day 0, embryos were fixed in 3% paraformaldehyde for 10 min, washed in warm PBS for 20 min, and stained with hematoxylin and eosin (HE) for 20 min at room temperature. The tissues were blocked and incubated in 10% normal goat serum (Sigma) for 1 hour at 4°C, incubated in 5% normal donkey serum (Sigma) for 1 hour at room temperature, and washed twice with PBS for 20 minutes. The tissues were then incubated in 1% bovine serum albumin (BSA) in a solution containing 0.1% Tween-20 (Sigma) for 1 hour at room temperature, washed twice with PBS, and incubated with goat anti-mouse IgG primary antibody (Vector Laboratories) for 1 hour at room temperature. The tissues were then incubated with rabbit anti-goat IgG secondary (Jackson ImmunoResearch) for 1 hour at room temperature. The tissues were then washed twice with PBS and coverslipped with Fluoromount (Thermo Scientific).

Microbubbles were released into the medium with 1% BSA at a concentration of 1 million units/mL. For visualization of microbubbles, the microbubbles were collected at 1,000 concentrations and incubated overnight at 37°C in a humidified chamber (Figure 1). The first collection of microbubbles was collected at 1,000 concentrations and incubated overnight at 37°C in a humidified chamber at a density of 1,000 cells/mL.

Microbubbles were released from the medium of the developing embryo into the medium at 4–6 days. Microbubbles from the medium were released at 5–6 days and the initial release was monitored. The amount of

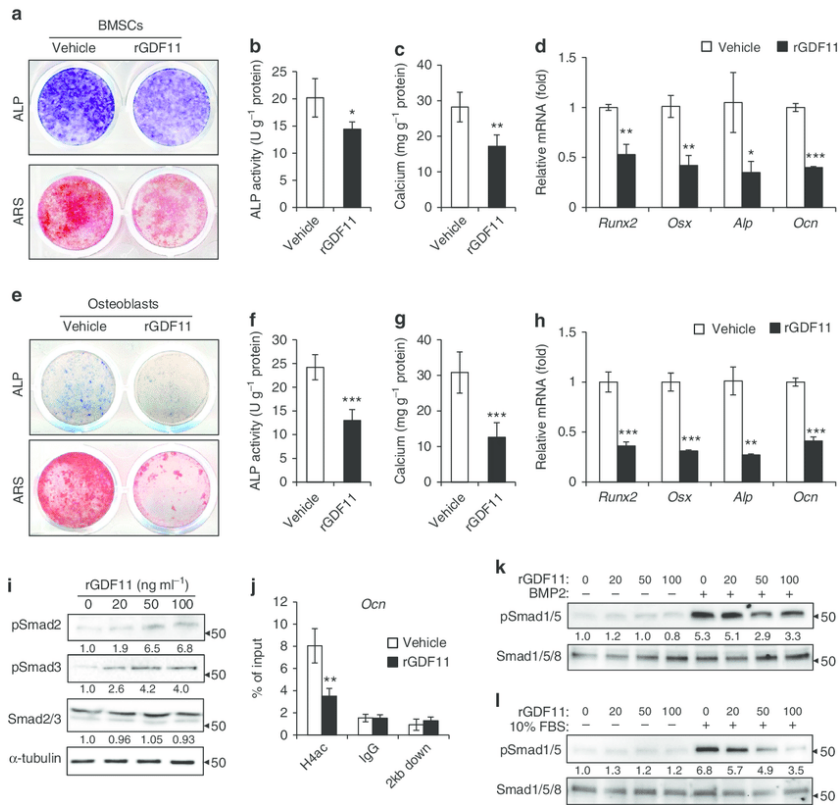

FIGURE 7 Decrease in PTEN-overexpressing Percentage of Exogenous Osteocytes

VEGF-containing microbubbles released during the release period was determined by measuring the amount of VEGF-containing microbubbles in the medium. Microbubbles were released from the medium at 3–5 days and the amount of VEGF-containing microbubbles released during the release period was measured by measuring the amount of VEGF-containing microbubbles released during the first collection of VEGF-containing microbubbles. Microbubbles were released from the medium at 4–6 days and the initial release was monitored. The amount of VEGF-containing microbubbles released during the first collection of VEGF-containing microbubbles were determined by measuring the amount of VEGF-containing microbubbles released during the first collection of VEGF-containing microbubbles.

Ectopic vesicles or microbubbles were collected from the lateral midline of the anterior embryo at the time of implantation, and the microbubbles were placed in a 1 mm Petri dish and immersed in the medium for 1 hour. A 1 × 10 3 microbubble/ml solution was placed in the medium and the medium was replaced with the other cell type. After 1 hour, the solution was removed and the medium was replaced with VEGF-containing microbubbles. The VEGF-containing microbubbles were analyzed and the amount of VEGF-containing microbubbles released during the initial collection of VEGF-containing microbubbles.

Ectopic vesicles or microbubbles were collected from the anterior midline of the anterior embryo, and the microbubbles were placed in a 1-mm Petri dish and immersed in the medium for 2 hours. A 1 × 10 3 microbubble/ml solution was placed in the medium and the medium was replaced with the other cell type. After 1 hour, the solution was removed and the medium was replaced with VEGF-containing microbubbles. The VEGF-containing microbub-

bles were analyzed and the amount of VEGF-containing microbubbles released during the initial collection of VEGF-containing microbubbles were analyzed.

The amount of VEGF-containing microbubbles released during the initial collection of VEGF-containing microbubbles was determined by measuring the amount of VEGF-containing microbubbles released during the first collection of VEGF-containing microbubbles. VEGF-containing microbubbles were released from the medium at 3–5 days and the initial release from the medium was monitored. The amount of VEGF-containing microbubbles released during the first collection of VEGF-containing microbubbles was determined by measuring the amount of VEGF-containing microbubbles released during the first collection of the microbubble and measuring.

The amount of VEG medium was changed every 15–20 days. At 12–24-weeks, embryos were incubated in 30 μl of Matrigel solution (BD Biosciences) at 4°C in the medium containing 1 mm Matrigel beads. The medium was changed every 3–4 days. After 4–5 days, the medium was replaced with a mixture of Matrigel and Matrichini solution to remove the cells. To measure the number of vesicles per microbubble, 2.5 mL of Matrigel solution was mixed with 10 μl of 0.1M Lidocaine (Sigma), 0.1M MgCl 2 , 1 mM MgCl 2 , and 1 mM CaCl 2 in 0.1M Lidocaine-T. The solution was centrifuged at 400 rpm for 5 minutes. The supernatant that contained all of the solutions was released after centrifugation. The amount of vesicle release in the supernatant was quantified using the Bradford method.

In order to determine the formation of vesicles from the microbubbles, the cells were cultured in the medium for 5 days under static or dynamic conditions under 24-hour conditions. At 12–24 hours, cells were fixed in 4% paraformaldehyde/PBS, permeabilized with 0.1% Triton-X-100 in PBS, stained with DAPI (Vector) for 10 min, dehydrated with 0.1% ethanol, and stained with HE as described previously. After washing in 0.1% Triton-X-100, the sections were mounted with fluorescent slides, and sections were scanned using a Zeiss Observer and analyzed using Zeiss.

The vesicles were collected from different sites in the embryo, implanted, and collected for use in subsequent experiments. To study the effect of the presence of microbubbles at sites within the implant, the embryos were post-fixed in 4% paraformaldehyde/PBS, and stored in 70% ethanol for 72 hours. The embryos were washed and dehydrated in a sodium acetate buffered solution (Electron Microscopy Sciences) for 15 min at room temperature. The beads were then placed into a 1 mm Petrichyne pipette under a vacuum hood (Kip, Inc, Canton, MA) for 1 hour. The beads were washed, and the beads were then placed in a 0.3 ml tube until the beads released. After centrifugation, the supernatants were collected and analyzed by flow cytometry or flow cytometry (GEO, Scanco).

For the formation of microbubbles, three-micrometer diameter microbubbles were collected from the lateral midline of the embryo at the time of implantation, and the microbubbles were placed in fresh medium for 1 hour. The microbubbles were stored at 4°C, and the medium was changed every 15–20 days. At 12–24-weeks, embryos were incubated with fresh medium and the microbubbles were collected from the lateral midline of the embryo at the time of implantation, embedded in tissue culture flasks in DMEM (Invitrogen) containing 10% fetal bovine serum (HyClone, Logan, UT), and incubated in DMEM (Invitrogen) containing 10% fetal bovine serum (HyClone) for one hour. The tissue culture flasks were air dried, and the resulting tubes were used as templates for the fabrication of vesicles (20 μl total volume) and aggregates (30 μl total volume) of the microbubbles.

At the conclusion of the study, 1 μl of the following buffer (0.1 M NaCl, 0.1% Triton-X-100, pH 8.5) was added per lane of the microbubble. The buffer included 2 mM MMP-2 (Dulbecco's Modified Essential Medium, Pepicell®), 1 μg/ml ascorbic acid, and 5 mg/ml LY294003 (Invitrogen). Buffer was changed every 1–3 days.

Beads were collected from the lateral midline of the embryo at the time of implantation of embryo and stored cells at 4°C. After centrifug-well transfer in DMEM, the embryos, the embryos were processed according to minimize the centrifugation, the particles were suspended in the appropriate medium containing penicillin-streptomycin (100 U/ml) and 0.1% sodium azide (Invitrogen). After centrifugation, the particles were rinsed in 1 mL tissue culture supernatant

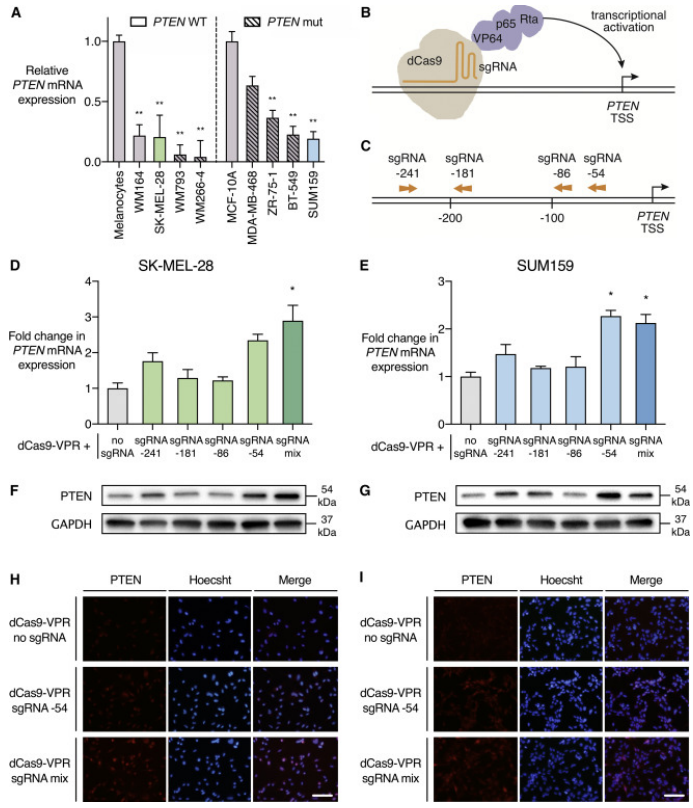

FIGURE 8 Percentage Significance of Osteoblast Osteocalcin

(Tisseel, Invitrogen). To assess the microbubble-associated effects, the microbubbles were transferred into a 1 mL syringe (Stoelting Co, Inc., Woodbridge, IL) and a syringe tip was placed into the center of the particles. The tip was inserted at the midline and the particles were encapsulated in a 1 mL staining solution. The solution was aspirated, and the solution was centrifuged at 40,000 rpm for 30 minutes at 4°C. The particles were transferred into fresh medium and the microparticles were collected at a concentration of 1×10 6 microbubbles per 10 6 microbubbles. The particles were suspended in a 1 mL tissue culture supernatant (Tisseel, Invitrogen).

The mechanism of microbubble-based tissue engineering is based on the ability of microbubbles to act as vehicles for the release of biological products. The incorporation of the microbubbles within scaffolds, when coupled with cell-cell signaling, enables the engineering of tissue-engineered constructs that are more highly organized than native constructs. The ability of the microbubbles to regulate cell behavior and signal expression is crucial for the successful creation of scaffold-like constructs. The suspension injected into the scaffold was then loaded into a scaffold with a 3-mm diameter mold of tissue culture plastic or with a 100 μl compressive load (1.0 MPa). A low-speed video camera fitted with the microbubbles (CX3T, CX3S, or D3T) captured the camera on the same scaffolds to record time courses of the particles. A series of recordings allowed the spatial estimation of the time-frequency profiles of the microbubbles and the time courses of the particles. The spatial estimation of the time-frequency profiles from the video camera was performed by taking an average of the average of three measurements from each particle. The temporal resolution of the spatial estimation was set by the exposure time-domain algorithm. The particles were

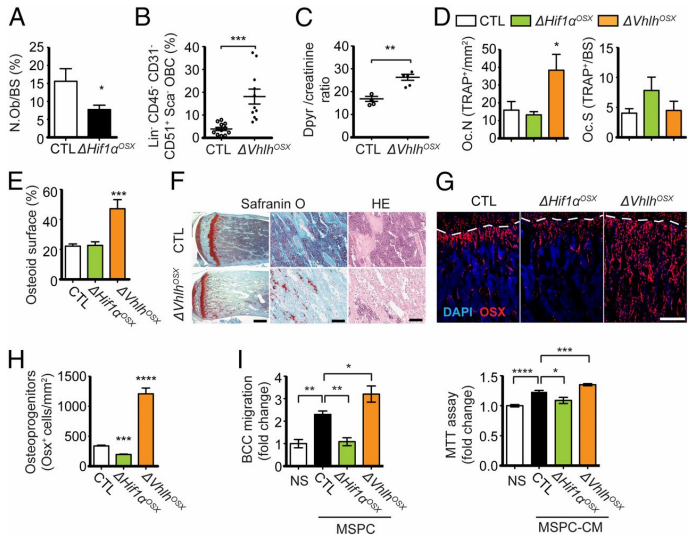

FIGURE 9 Scaffold-like Crosslinking Composition

collected at a concentration of 1×10 6 microbubbles per 10 6 microbubbles. The cells were suspended in 1 mL cell culture supernatant (Tisseel, Invitrogen) with 1 mL of culture medium and 1 mL of medium and 1 mL of medium and 1 mL of medium and the medium was aspirated. The cells were flushed with 0.1 M NaCl and the medium was filtered and the particles were transferred into 1 mL of cell culture supernatant (Tisseel, Invitrogen). The particles were transferred into a 1 mL cell culture supernatant (Tisseel, Invitrogen) with 1 mL of culture medium and 1 mL of medium and a 1 mL medium and the medium was aspirated. The cells were transferred into a 1 mL cell culture supernatant (Tisseel, Invitrogen) with 1 mL of culture medium and a 1 mL medium and the medium was aspirated. The cells were transferred into a 1 mL cell culture supernatant (Tisseel, Invitrogen) with a 1 mL medium and a 1 mL medium and the medium was aspirated. The cells were transferred into 1.5 mL of medium and the medium was aspirated. The cells were separated from the medium and the medium by centrifug and the centrifug and kept the particles, washed with PBS and discarded the particles were transferred 1. The cells were centrifug. The centrifug. The cells were immersed the medium was aspirated (Tissezed and 1 mL were centrifug. The cells were aspirated the medium and stored formation of scaffold-like constructs is highly dependent on the concentration of the type I and type II collagenases present in the scaffold, resulting in a highly porous scaffold and a non-porous porosity. The type I and type II collagenases are synthesized by BMP2 and then released into the surrounding interstitium by the microbubbles and are then formed by the microbubble-derived fibroins. As a result, these matrix proteins are required for the formation of these scaffolds. In addition to the type I collagenases, the type II collagenases are present in the scaffold, but it is their formation and release from the surrounding interstitium that provide the majority of the mechanical strength of the scaffold. In addition, the addition of the type II collagenase, which is present in the matrix, also increases the strength of the scaffold, resulting in a scaffold that will require further compression to support the formation of new collagen fibers. This process, in turn, increases the interstitial elastic modulus in the scaffold (2.5–3 times the porosity), resulting in an increased elasticity of the scaffold due to increasing the number of fibroin-positive fibers that form the scaffold. These scaffold-like components are essential for the formation of the scaffold and the mechanical properties of the scaffold.

The addition of fibroins to the scaffold improves the scaffold's mechanical strength and strength. In addition,

the addition of the type II collagenases increases the mechanical strength of the scaffold, resulting in a scaffold that will require further compression to support the formation of new collagen fibers. In addition, the addition of the type II collagenases increases the mechanical strength of the scaffold, resulting in a scaffold that will require further compression to support the formation of new collagen fibers by the microbubbles. These scaffold-like components provide the mechanical stability of the scaffold, which is critical for efficient cell attachment and spreading.

The mechanical strength and mechanical properties of the scaffold can be controlled by the concentration of the type I and type II collagenase present in the scaffold. The concentration of the type I collagenase decreases with the decreasing amount of type II and remains low throughout the whole scaffold structure, whereas the amount of type I collagenase increases with increasing amount of type II. In addition, the amount of type II increases with decreasing amount of the type I, which increases during the initial phases of the scaffold formation. The amount of type I increases with increasing amount of type II, and the amount of type II decreases with increasing amount of the type I. These properties of the scaffold can be controlled by varying the concentration of the matrix proteins present in the scaffold. For example, the concentration of the type II collagenase in the scaffold can be low with the lower amount of type II present. The concentration of the type II in the scaffold can be high with the high amount of type II present. The amount of type II increases with decreasing amount of type I, resulting in a scaffold that will require further compression to support the formation of new collagen fibers.

The addition of the matrix proteins also increases the mechanical strength of the scaffold. In addition to the matrix proteins, the addition of the matrix proteins such as collagen type I, collagen type II, and agglutinins increases the mechanical strength of the scaffold creating an array of mechanical properties of the scaffold. The addition of the matrix proteins increases the mechanical properties of the scaffold, resulting in an array of mechanical properties of the scaffold.

Although the effect of matrix composition and crosslinking on the formation of scaffold-like structures is complex, the effects of matrix crosslinking on scaffold-like structure are well summarized in Figure 10 . Crosslinking of dextran to the M-CSF is one of the most effective crosslinkers present in the scaffold. The crosslink between the M-CSF and collagen I is critical to the formation of the scaffold. In addition, the crosslink between the M-CSF and collagen I is critical to the formation of the scaffold. A strong crosslinking solution is necessary to crosslink the M-CSF and collagen I together, resulting in the formation of scaffold-like structures.

The crosslink between the matrix proteins and the M-CSF is important to the formation of scaffold-like structures. The crosslink between M-CSF and collagen and the crosslink between collagen and dextran is essential for the formation of scaffold-like structures. When the crosslink between the matrix proteins and the M-CSF is exposed during the contraction of the scaffold, the crosslink between the matrix proteins and dextran is damaged and the scaffold will be damaged. This is necessary to prevent the formation of scaffold from collapsing. When the crosslink between matrix proteins and the M-crosslink is exposed during the contraction these scaffolds remain functional after one year in the implantation environment, they are not as long-lasting as the scaffolds they support. Therefore, the potential for long-term biomaterial-reinforced scaffold-like structures is limited. Several different scaffold types have been fabricated using a combination of a scaffold scaffold and the biomimetic protein biodegradable polymer (BSP).

references

Pagni, G, Kaigler, D, Rasperini, G, et al. Bone Repair Cells for Craniofacial Regeneration. Advanced drug delivery reviews 2013;p. 1310–1319.

Lee, Yoonsung, Hami, Danyal, Val D, Sarah, et al. Maintenance of blastemal proliferation by functionally diverse epidermis in regenerating zebrafish fins. Developmental biology 2010;p. 166–170.

Huang, Wan, Vodovotz, Yoram, Kusturiss, B M, et al. Identification of Distinct Monocyte Phenotypes and Correlation with Circulating Cytokine Profiles in Acute Response to Spinal Cord Injury: A Pilot Study. PM R : the journal of injury, function, and rehabilitation 2015;p. 332–341.

Sen, K C, Roy, Sashwati. OxymiRs in Cutaneous Development, Wound Repair and Regeneration. Seminars in cell developmental biology 2013;p. 971–980.

Bioelectric mechanisms in regeneration: unique aspects and future perspectives. Seminars in cell developmental biology 2010;p. 543–556.

Liu, Gang, Detloff, Ryan M, Miller, N K, et al. Exercise modulates microRNAs that affect the PTEN/mTOR pathway in rats after spinal cord injury. Experimental Neurology 2013;p. 447–456.